


Control of the size and luminescence of carbon nanodots by adjusting ambient pressure in laser ablation process

Cite as: J. Appl. Phys. **127**, 083102 (2020); <https://doi.org/10.1063/1.5128042>

Submitted: 17 September 2019 . Accepted: 11 February 2020 . Published Online: 27 February 2020

Xiaoyu Li, Lihe Yan , Jinhai Si, Yanmin Xu, and Xun Hou



View Online



Export Citation



CrossMark

Lock-in Amplifiers
Find out more today



 Zurich
Instruments



Control of the size and luminescence of carbon nanodots by adjusting ambient pressure in laser ablation process

Cite as: J. Appl. Phys. 127, 083102 (2020); doi: 10.1063/1.5128042

Submitted: 17 September 2019 · Accepted: 11 February 2020 ·

Published Online: 27 February 2020



Xiaoyu Li, Lihe Yan,^{a)}  Jinhai Si, Yanmin Xu, and Xun Hou

AFFILIATIONS

Key Laboratory for Physical Electronics and Devices of the Ministry of Education and Shaanxi Key Lab of Information Photonic Technique, School of Electronics and Information Engineering, Xi'an Jiaotong University, Xi'an 710049, China

^{a)}Author to whom correspondence should be addressed: liheyang@mail.xjtu.edu.cn

ABSTRACT

A femtosecond pulse laser was used to fabricate carbon nanodots (CDs), of which the particle size and photoluminescence (PL) properties could be effectively controlled by adjusting ambient pressure. By increasing the reaction pressure, the particle size of CDs gradually decreased and finally reached less than 1 nm at 4 MPa. Simultaneously, the fluorescence intensity of the CDs first increased and then decreased by further increasing the pressure. By examining the PL dynamics and the chemical structure of the CDs, we found that the PL change of products was attributed to the quantity change of functional groups attached to the CDs due to the surface area change of the carbonic core.

Published under license by AIP Publishing. <https://doi.org/10.1063/1.5128042>

I. INTRODUCTION

Photoluminescent carbon nanodots (CDs) are discrete quasi-spherical nanoparticles with a size less than 10 nm, the particle surface sites of which are passivated by surface functionalization.^{1–3} Since they were first discovered in 2004, CDs have attracted increasing attention due to their photostability, stable photoluminescence (PL),^{4,5} high water solubility, excellent biocompatibility, low toxicity, and good chemical stability.^{6–12} To date, different kinds of CDs have been fabricated by a number of methods due to their special properties and extensive applications, such as electrochemical etching, plasma treatment, microwave assisted synthesis, hydrothermal method, ultrasonic method, and porous template method.^{4,9,13,14} Generally, the size of the CDs can be controlled by changing the reaction conditions, further strictly affecting their PL properties.¹⁵

The laser ablation in solution (LAS) method is a fast, cheap, and clean way to synthesize CDs.^{16–20} The reaction mechanism of nanomaterials prepared by the LAS method can be explained by the Coulomb explosion model.²¹ When a femtosecond laser pulse with ultrahigh peak power density is injected into the target, the ablated area could be highly ionized to form high temperature and high pressure plasma plumes. In the local area where the laser is

focused, the temperature can exceed 10 000 K, and the pressure can exceed 20 GPa. The plasma plume undergoes explosive splitting under strong Coulomb forces to produce nanoparticles.^{22,23} In the preparation of nanomaterials by laser deposition, vacuum pressure plays an important role in the evolution of the plasma plume, which has often been used to control the morphology of the products.^{14,24} However, the effect of ambient pressure on the size and PL of the nanodots fabricated using the LAS method has not been reported, although the influence of other parameters such as laser power, spot size, and irradiation time on the size and the PL properties have previously been studied.¹⁵ As the particle size and the PL properties of the luminescent nanodots are very important features of the materials, and severely limit their potential applications,²⁵ it is very important to study how to control the size and PL of CDs by adjusting the ambient pressure in the LAS process.

In this work, different ambient pressures are applied during the synthesis of CDs by femtosecond laser ablation, and finally CDs less than 1 nm are obtained at a pressure of 4 MPa. Meanwhile, the PL intensity of the CDs first increases and then decreases by further increasing the pressure. The reduction in the size of CDs results in the change of the surface area of the carbon core, and the number of functional groups attached to the CDs

changes causes the PL change of the CDs. The results suggest that changing the pressure is a versatile and simple method to synthesize CDs with adjustable size and PL properties.

II. EXPERIMENTAL SECTION

In the preparation, 50 mg of carbon particles with an average size of 40–400 nm was dispersed into 50 ml of *N*-methyl pyrrolidone (NMP). After ultrasonic treatment and dilution, about 10 ml of the suspension was used for laser irradiation in an autoclave. The sealed autoclave reactor was connected with a gas cylinder filled with nitrogen, and the pressure in the reactor could be adjusted from atmosphere to 4 MPa. A quartz optical window was embedded in the cover of reactor, passing through which the laser beam could be focused in the solution.

During the ablation process, a Ti: sapphire femtosecond pulse laser with a center wavelength of 800 nm was used. The repetition rate is 1 kHz and the pulse duration is 150 fs. The solution was ablated using laser pulses of 400 μ J power for 0.5 h and the ambient pressure was adjusted from atmosphere to 4 MPa, respectively. The mixture was centrifuged after laser irradiation process to remove large particles, and finally supernatant containing the desired CDs was obtained.

Transmission electron microscopy (TEM) and high-resolution TEM (HRTEM) were conducted on a JEM-2100Plus microscope to measure the particle size and lattice structure. X-ray photo-electron spectroscopy (XPS) spectra were obtained using a Thermo Fisher ESCALAB Xi+ XPS system. Absorption and PL spectra of the CDs were measured using a UV-2600 and FLS920 (Edinburgh) spectrophotometer. Fourier transform infrared (FTIR) spectra were obtained from a VERTEX 70 instrument. Time-resolved PL (TRPL) data of CDs were measured by a time-correlated single-photon counting (TCSPC) system with a 404 nm picosecond LED as the excitation source. All the PL and TRPL spectra were measured at atmospheric pressure. X-ray diffraction (XRD) patterns of the samples were obtained by using an x-ray diffractometer with Cu $K\alpha$ radiation ($\lambda = 0.15406$ nm).

III. RESULTS AND DISCUSSION

First, we studied the effect of ambient pressure on the size of the products. Figure 1(a) shows the TEM image of CDs prepared at atmosphere, while Figs. 1(b) and 1(c) show those prepared at 2.5 MPa and 4 MPa, respectively. It can be seen that the prepared CDs are uniformly dispersed in the solution without agglomeration. The HRTEM images of CDs given in the insets of Figs. 1(a)–1(c) show the same lattice spacing, which is 0.21 nm and almost

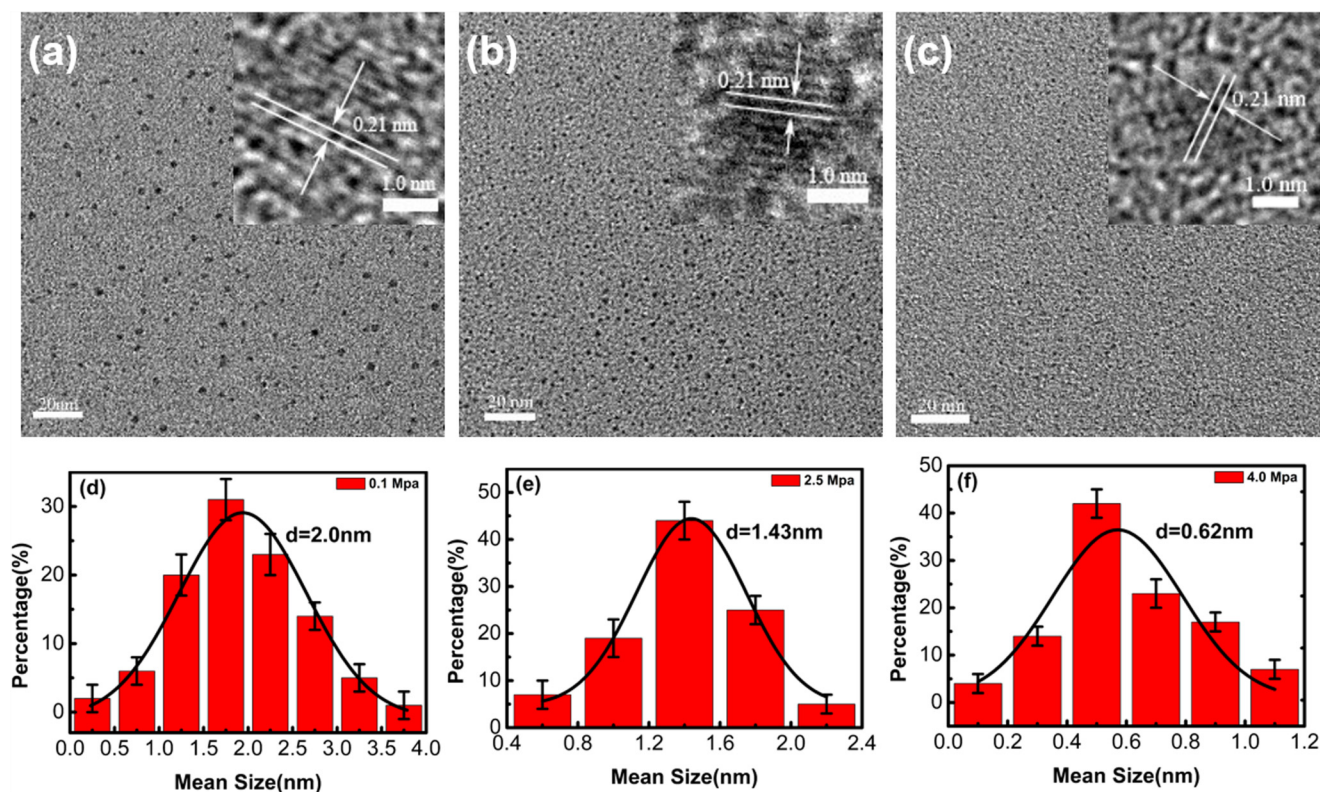


FIG. 1. TEM images of CDs at (a) atmosphere, (b) 2.5 MPa, and (c) 4 MPa. The corresponding size distributions of CDs at (d) 0.1 MPa, (e) 2.5 MPa, and (f) 4.0 MPa.

identical with the (111) plane of graphite.¹⁷ Figures 1(d)–1(f) correspond to the size distribution of CDs prepared at different pressures, respectively. The average sizes of the CDs are estimated to be 2.0, 1.43, and 0.62 nm, respectively. The results suggest that the pressure of the solutions will influence the size of CDs, which will be reduced to even less than 1 nm as the pressure is increased.

In the laser ablation process, when the femtosecond laser is injected into the solution, the irradiated local area will generate an extremely high temperature, which will result in high ionization of the material and the generation of plasma.^{21,26} The expansion of the plasma further produces bubbles, which contain various molecules and atoms produced by decomposition of the solution and vaporization of the target.^{27–29} While the plasma is expanding, the surrounding liquid continuously compresses the plasma and transfers the energy in the bubble, lowering the temperature of the plasma.²⁹ In this process, various chemical reactions take place, and the nucleation and growth of the nanomaterials continue. Finally, nanoparticles with different sizes may be produced in the bubbles.^{30,31} When the ambient pressure of the surrounding liquid is increased, the compression effect on the plasma could be enhanced, and the cooling rate is accelerated. As a result, the growth time of the CDs is shortened, and the size of the products is remarkably reduced.

Furthermore, we measured the influence of the ambient pressure on the PL intensity. According to the typical emission spectra of CDs at atmospheric pressure and 2.5 MPa [Figs. 2(a) and 2(b)], CDs show the maximum excitation and emission wavelengths around 380 and 470 nm, respectively. Although the emission spectra are independent of the applied pressure, the emission intensity changes significantly with the change of pressure. The emission

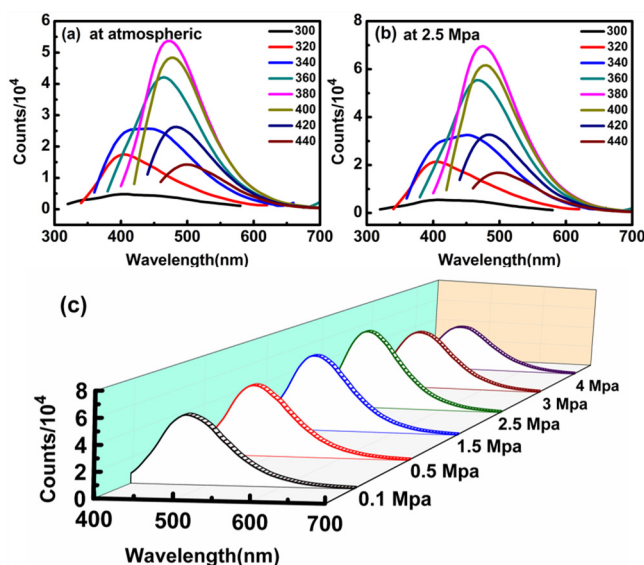


FIG. 2. Emission spectra of CDs at (a) atmosphere and (b) 2.5 MPa excited at different wavelengths. Emission spectra excited at 380 nm of CDs at (c) 0.1–4.0 MPa.

spectra excited by 380 nm of CDs prepared at different pressures [Fig. 2(c)] show that the PL intensity increases with the increase of pressure first, and then decreases after 2.5 MPa.

The UV-Vis absorption, FTIR, and TRPL spectra of CDs were measured to explain the PL change of the CDs. The spectra show a strong absorption peak at about 260–285 nm [as shown by Fig. 3(a)], which is derived from the π - π^* transition of aromatic sp^2 domains.³² There is a broad absorption band around 340 nm attributed to the n - π^* transition of the C=O band.³³ By increasing the ambient pressures, the absorption increases significantly. However, after the pressure reaches 2.5 MPa, the absorption decreases, as given in the inset of Fig. 3(a), agreeing well with the PL intensity change of the samples. From the FTIR spectrum of the CDs [Fig. 3(b)], it can be seen that all CDs prepared at different ambient pressures exhibit the same characteristic bonds including the vibration of C=O at 1630 cm^{-1} ,³⁴ C–H vibrations at around 2920 and 1470 cm^{-1} ,³⁵ and stretching vibration of O–H bond at 3420 cm^{-1} .³⁴

To explore the origin of the PL, we measured the PL dynamics of the CDs prepared at atmosphere. Figure 3(c) indicates the TRPL curves at different emission wavelengths (excited by 404 nm light) of the CDs prepared at atmosphere. All the decay curves can be well fitted using a double-exponential function, and a fast decay process of 1.8 ns and a slow decay process of 12.0 ns are observed. For the emission at wavelengths of 460, 480, and 500 nm, the average lifetimes of the PL increase from 6.2 ns to 6.5 ns and 7.1 ns. The average lifetimes of the PL increase with increasing emission wavelength because of the increments of the ratio of the slow decay process. These results are in accordance with the previous reports, in which the fast decay process is due to the direct excitation–combination of the carriers on the surface state, while the slow decay may be due to the relaxation of the carriers from the excited carbon nuclei to the surface groups:^{36–38} the different surface functional groups (C=O, C–H, and O–H) will form different surface state energy levels; the carbonic core and the surface state could be excited simultaneously at 404 nm excitation; and the relaxation from the carbonic core onto the surface state and the direct radiative recombination on surface states correspond to the slow and fast decays, respectively. With increasing the emission wavelength, the corresponding surface state energy level is lower, and the proportion of the slow decay from the carbonic core to the emission surface states is larger, causing the prolonging of the decay time of the PL. Figure 3(d) shows the PL dynamics at 480 nm (excited by 404 nm light) of the CDs prepared at different pressures. We can see that the emission of CDs at different pressures shows almost the same temporal behavior and the decay process does not change with changes in pressure. These results indicate that the PL of all the CDs prepared at different pressures is originated from the surface functional groups. The PL intensity change of the samples is due to the quantity of the surface functional groups rather than the type.

To confirm our suspicions above, XPS analysis was used to demonstrate the differences in surface functional groups of CDs prepared at different pressures. The C1s spectrum of CDs [Fig. 4(a)] indicates three peaks corresponding to C=C bond at 284.5 eV, C–O bond at 286.0 eV, and C=O bond corresponding to the peak at 287.9 eV.³⁴ The content of the three bonds is calculated to be about 89.0%, 5.76%, and 5.24%, respectively. As given in

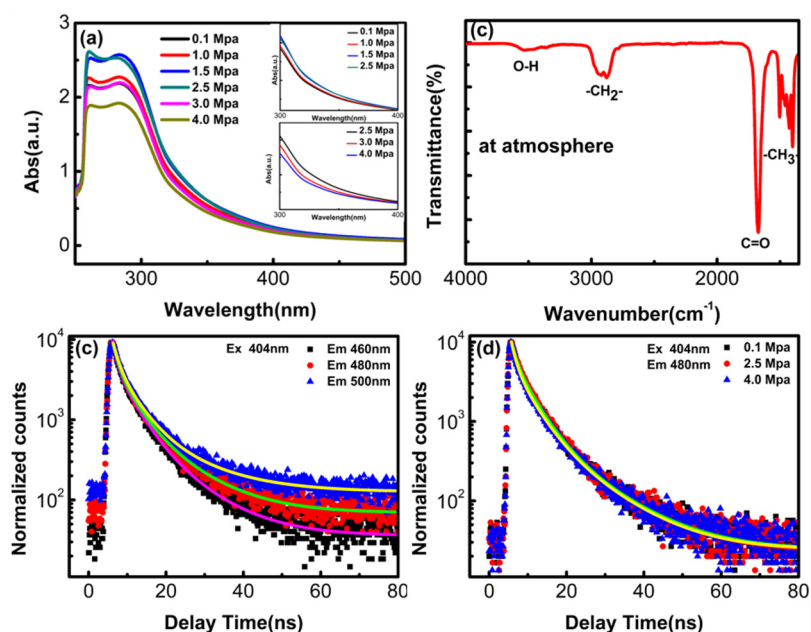


FIG. 3. UV-Vis absorption spectra of CDs by (a) 0.1 to 4.0 MPa. (b) FTIR spectra of the CDs prepared at atmosphere. (c) PL dynamics excited by 404 nm light of the CDs prepared at atmosphere. (d) PL dynamics at 480 nm of CDs at different pressures.

Figs. 4(b) and 4(c), when the ambient pressure is changed, the proportion of the C—O and C=O bonds is also changed, indicating the quantity difference of the surface groups. Figure 4(d) summarizes the dependence of the proportion of the C—O and C=O in C1s spectrum on the ambient pressure. The results show that these groups increase significantly when the pressure is 2.5 MPa and decrease when the pressure is further increased.

Based on the discussions above, we can conclude that the PL intensity change of the CDs prepared at different pressures is originated from the change of the quantity of the functional groups. In our experiments, when the pressure is increased, the size of the CDs is decreased, and the ratio of the surface area to the volume of the CDs could be increased. As a result, the proportion of the surface functional groups increases and the luminescence intensity

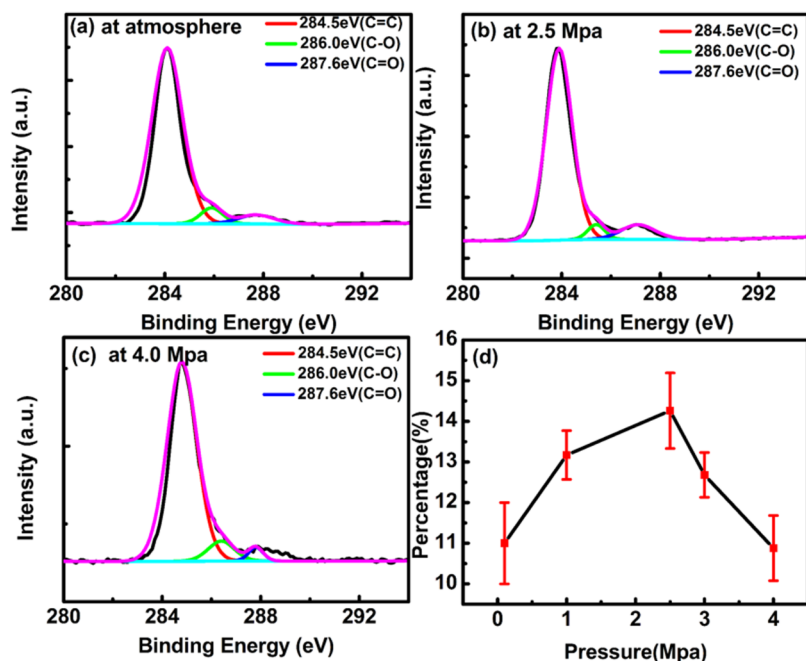


FIG. 4. High-resolution C1s XPS spectra of CDs at (a) atmosphere and (b) 2.5 MPa. (c) 4.0 MPa. (d) The proportion of CDs surface functional groups (C—O/C=O bonds) at different pressures.

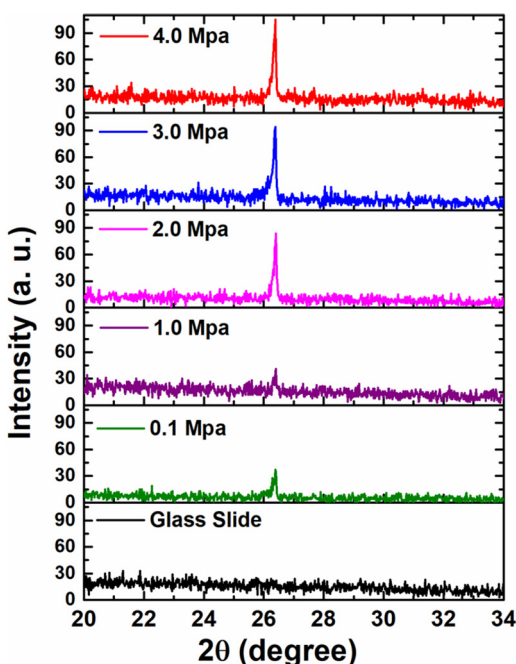


FIG. 5. XRD patterns of the CDs prepared at different pressures.

is enhanced. When the pressure is further increased, the size of the CDs sharply decreases. As the ultrasmall carbonic core could be well crystallized, the surface site for the attachment of functional groups could be decreased, causing the reduction of the PL intensity. Figure 5 shows the XRD patterns of the CDs prepared at different pressures. The spectrum of the CDs has an obvious peak around 26° corresponding to the (002) planes of graphite. The peak intensity of the CDs prepared at low external pressure of 1 MPa changes slightly compared with those fabricated at atmosphere. However, sharp XRD peaks appear when the pressure is higher than 2.0 MPa, and the intensity increases with an increase in pressure, indicating a better crystalline structure of the carbonic core. The higher crystallization of core might hinder the attachment of surface groups, causing the decrease of the PL intensity of the CDs.

IV. CONCLUSIONS

The effect of ambient pressure on the size and PL property of CDs is investigated in this paper. The size of the CDs can be effectively reduced to even less than 1 nm as the pressure is increased. The PL intensity increases with an increase in pressure first and then decreases with a further increase in pressure. When the size of the CDs is decreased, the ratio of the surface area to the volume of the CDs could increase. As a result, the proportion of the surface functional groups increases and the luminescence intensity is enhanced. As the ultrasmall carbonic core could be well crystallized, the surface site for the attachment of functional groups could decrease, causing the reduction of the PL intensity. Our results

indicate that the number of surface functional groups of CDs is related to its size, which in turn affects the PL of the CDs.

ACKNOWLEDGMENTS

This work is supported by the National R&D Program of China (2017YFA0207400); National Natural Science Foundation of China (Grant Nos. 11674260 and 61690221); Fundamental Research Funds for the Central Universities (No. xjj2017189); and the Key research and Development Program of Shaanxi Province (Grant No. 2017ZDXM-GY-120).

REFERENCES

- X. T. Zheng, A. Ananthanarayanan, K. Q. Luo, and P. Chen, *Small* **11**, 1620–1636 (2015).
- Y. P. Sun, B. Zhou, Y. Lin, W. Wang, K. A. Fernando, P. Pathak, M. J. Meziani, B. A. Harruff, X. Wang, H. Wang, P. G. Luo, H. Yang, M. E. Kose, B. Chen, L. M. Veca, and S. Y. Xie, *J. Am. Chem. Soc.* **128**, 7756–7757 (2006).
- L. Cao, X. Wang, M. J. Meziani, F. Lu, H. Wang, P. G. Luo, Y. Lin, B. A. Harruff, L. M. Veca, D. Murray, S. Y. Xie, and Y. P. Sun, *J. Am. Chem. Soc.* **129**, 11318–11319 (2007).
- S. N. Baker and G. A. Baker, *Angew. Chem. Int. Ed. Engl.* **49**, 6726–6744 (2010).
- S. Y. Lim, W. Shen, and Z. Gao, *Chem. Soc. Rev.* **44**, 362–381 (2015).
- P. Miao, K. Han, Y. Tang, B. Wang, T. Lin, and W. Cheng, *Nanoscale* **7**, 1586–1595 (2015).
- J. Bartelmeß, S. J. Quinn, and S. Giordani, *Chem. Soc. Rev.* **44**, 4672–4698 (2015).
- Q. Hao, J. Pang, Y. Zhang, J. Wang, L. Ma, and O. G. Schmidt, *Adv. Opt. Mater.* **6**, 1700984 (2018).
- J. Wang, F. Peng, Y. Lu, Y. Zhong, S. Wang, M. Xu, X. Ji, Y. Su, L. Liao, and Y. He, *Adv. Opt. Mater.* **3**, 103–111 (2015).
- H. Wang, Y. Xie, X. Na, J. Bi, S. Liu, L. Zhang, and M. Tan, *Food Chem.* **286**, 405–412 (2019).
- V. Nguyen, L. Yan, J. Si, and X. Hou, *Opt. Mater. Express* **6**, 312 (2016).
- V. Nguyen, L. Yan, H. Xu, and M. Yue, *Appl. Surf. Sci.* **427**, 1118–1123 (2018).
- H. Li, X. He, Y. Liu, H. Huang, S. Lian, S. Lee, and Z. Kang, *Carbon* **49**, 605–609 (2011).
- L. Tang, R. Ji, X. Cao, J. Lin, H. Jiang, X. Li, K. S. Teng, C. M. Luk, S. Zeng, J. Hao, and S. P. Lau, *ACS Nano* **6**, 5102–5110 (2012).
- V. Nguyen, L. Yan, J. Si, and X. Hou, *J. Appl. Phys.* **117**, 084304 (2015).
- D. Werner and S. Hashimoto, *J. Phys. Chem. C* **115**, 5063–5072 (2010).
- D. Tan, S. Zhou, B. Xu, P. Chen, Y. Shimotsuma, K. Miura, and J. Qiu, *Carbon* **62**, 374–381 (2013).
- D. Werner and S. Hashimoto, *Langmuir* **29**, 1295–1302 (2013).
- A. Menéndez-Manjón, B. N. Chichkov, and S. Barcikowski, *J. Phys. Chem. C* **114**, 2499–2504 (2010).
- D. Tan, B. Xu, P. Chen, Y. Dai, S. Zhou, G. Ma, and J. Qiu, *RSC Adv.* **2**, 8254 (2012).
- G. Yang, *Prog. Mater. Sci.* **52**, 648–698 (2007).
- D. Werner, A. Furube, T. Okamoto, and S. Hashimoto, *J. Phys. Chem. C* **115**, 8503–8512 (2011).
- D. Tan, S. Zhou, J. Qiu, and N. Khusro, *J. Photochem. Photobiol. C* **17**, 50–68 (2013).
- Y. Suda, T. Ono, M. Akazawa, Y. Sakai, J. Tsujino, and N. Homma, *Thin Solid Films* **415**, 15–20 (2002).
- H. Ming, Z. Ma, Y. Liu, K. Pan, H. Yu, F. Wang, and Z. Kang, *Dalton Trans.* **41**, 9526–9531 (2012).
- V. Amendola and M. Meneghetti, *Phys. Chem. Chem. Phys.* **15**, 3027–3046 (2013).

- ²⁷A. De Bonis, M. Sansone, L. D'Alessio, A. Galasso, A. Santagata, and R. Teghil, *J. Phys. D Appl. Phys.* **46**, 445301 (2013).
- ²⁸A. De Giacomo, M. Dell'Aglio, A. Santagata, R. Gaudiuso, O. De Pascale, P. Wagener, G. C. Messina, G. Compagnini, and S. Barcikowski, *Phys. Chem. Chem. Phys.* **15**, 3083–3092 (2013).
- ²⁹Z. Yan and D. B. Chrisey, *J. Photochem. Photobiol. C* **13**, 204–223 (2012).
- ³⁰P. Wagener, S. Ibrahimkuttiy, A. Menzel, A. Plech, and S. Barcikowski, *Phys. Chem. Chem. Phys.* **15**, 3068–3074 (2013).
- ³¹L. Lavis, J. L. Le Garrec, L. Hallo, J. M. Jouvard, S. Carles, J. Perez, J. B. A. Mitchell, J. Decloux, M. Girault, V. Potin, H. Andrzejewski, M. C. Marco De Lucas, and S. Bourgeois, *Appl. Phys. Lett.* **100**, 164103 (2012).
- ³²Z. Luo, Y. Lu, L. A. Somers, and A. T. C. Johnson, *J. Am. Chem. Soc.* **131**, 898–899 (2009).
- ³³M. Chen, W. Wang, and X. Wu, *J. Mater. Chem. B* **2**, 3937–3945 (2014).
- ³⁴Z. Xu, L. Yang, X. Fan, J. Jin, J. Mei, W. Peng, F. Jiang, Q. Xiao, and Y. Liu, *Carbon* **66**, 351–360 (2014).
- ³⁵S. G. Osswald, V. Yushin, S. Mochalin, O. Kucheyev, and Y. Gogotsi, *J. Am. Chem. Soc.* **128**, 11635–11642 (2006).
- ³⁶V. Nguyen, J. Si, L. Yan, and X. Hou, *Carbon* **108**, 268–273 (2016).
- ³⁷V. Nguyen, J. Si, L. Yan, and X. Hou, *Carbon* **95**, 659–663 (2015).
- ³⁸A. Sciortino, A. Cannizzo, and F. Messina, *J. Carbon Res. C* **4**, 67 (2018).